IEEE Robotics and Automation Letters (RAL) paper presented at the
2020 IEEE/RSJ International Conference on Intelligent Robots and Systems (IROS)
October 25-29, 2020, Las Vegas, NV, USA (Virtual)

Communication Maintenance of Robotic Parasitic Antenna Arrays

Jeffrey N. Twigg[1], Nikhil Chopra[2], and Brian M. Sadler[1]

***Abstract*— Recent developments in low-VHF antenna design and parasitic antenna array research show it is possible to form multi-robot antenna arrays. These arrays have the potential to extend communication range in urban and indoor environments. However, existing control formulations are not general enough to support this new capability. We first propose a generalized version of a disk model that describes a parasitic array. This model is then integrated into a Fiedler maximization approach for maintaining communication. Through simulation, we test our approach and demonstrate its ability to increase communication range by increasing array size.**

Index Terms–Networked Robots, Cooperative Robots, Communication Maintenance, Antenna Arrays, Fielder value

I. INTRODUCTION

Multi-robot systems need to actively control agents to maintain connectivity when communications infrastructure is not present or reliable. Connectivity maintenance approaches often require motion control of *individual* robots to maintain communication within the robotic team. In this paper, we consider a different paradigm where the robotic systems are coordinated to create a wireless communications capability beyond that which can be achieved by individual robots. The research on low-VHF antennas has shown that robots, if correctly positioned, create a passively coupled antenna array which communicates farther than any of the agents could individually[1]. This directional robotic antenna array, as shown in Fig. 1b, is fundamentally different from a single antenna which creates an omni-directional beam pattern, as shown in Fig. 1a.

To exploit the parasitic coupling for an enhanced beam pattern, we seek to create a controller that guides a multi-robot system over long ranges. Specifically we utilize low-VHF antennas to form parasitic arrays to communicate over long distances (in the case we study, > 150 m). The objective of our controller is to maintain and improve the connectivity graph of these robotic agents. As shown in Fig. 1a, we denote the agents communicating at low-VHF as *active antenna agents*. Active antenna agents have low-VHF antennas that are electrically excited (i.e., connected to the radio onboard). There are also *passive antenna agents* which are robots that have low-VHF passive antennas and therefore require no low-VHF radio. As shown in Fig. 1b, one or more of these passive antenna agents reflect and spatially focus radiation around the active antenna agents. When properly configured, these agents form a parasitic antenna array. While the agents forming each parasitic array need to control frequency, antenna spacing, and antenna length, this is outside of the scope of this paper. The electromagnetics

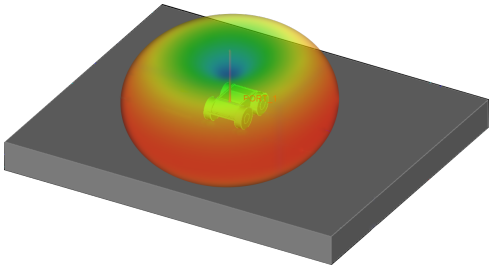

(a) Electromagnetic radiation of a single, low-VHF electrically small antenna mounted on a ground robot

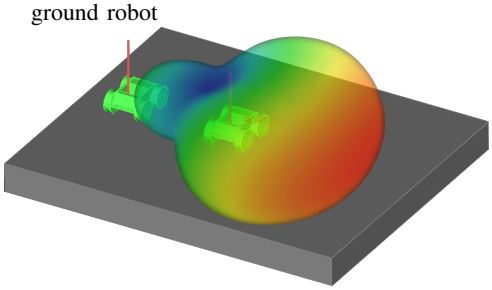

(b) Parasitic antenna array created by a second robot with a passive antenna that mutually couples with the antenna of the robot in Fig. 1a

Fig. 1: Simulation of low-VHF parasitic array forming robots [2] ©2019 IEEE

of the parasitic array, including optimization of the antenna placement, is considered in [2]. Here, we focus on the motion control problem of a multi-agent system to enable parasitic array formation so as to establish desired connectivity. Our contributions to solving this problem are the following:

- Introducing a variable state, called parasitic effect, for describing number of passive antenna agents in a parasitic Yagi-Uda array, a specific type of parasitic array.
- Creating a model of induced beam pattern as a function of number of agents.
- Formulating a Fiedler value maximization approach for groups of parasitic antenna arrays.
- Comparing connectivity maintenance with agents that can form parasitic arrays and those which cannot.

This work is a first step towards controlling a multi-robot system which can reliably communicate in non-line-of-sight (NLOS) environments using low-VHF, such as safety and rescue contexts (e.g., city building, cluttered outdoor, and urban settings). This is especially important in complex environments, enabling the multi-robot collective to establish and maintain a network topology.

In Section II we place our research in the context of existing work. Section III describes our model for parasitic

[1]CCDC Army Research Laboratory, Adelphi, MD 20783
[2]Department of Mechanical Engineering, University of Maryland, College Park, MD 20742

arrays in terms of gain, and the basics of maximizing Fiedler to improve connectivity in a multi-robot network. With this foundation, we discuss how to create a multi-agent controller for robotic parasitic arrays. Next, we present simulations using this controller in Section IV. Finally, we discuss our conclusions and future work in Section V.

II. Related Work

The typical approach for multiple agents to maintain communications is to mobilize robots for the purpose of relaying signals [3][4] or planning for periodic communication [5]. Researchers have also explored controlling other degrees of freedom for maintaining communication by adapting transmission power [6], changing coding [7], actuating directional antennas [8][9], and changing frequency [10]. The majority of research in communication maintenance is at industry standard WiFi frequencies (e.g., 2.4 GHz, 5 GHz). Unfortunately, in complex/dense environments (i.e., indoors, urban areas) the received signal strength (RSS) at this frequency varies rapidly with position and time due to multipath fading. Mobility planning approaches for maintaining LOS among agents help to avoid issues with NLOS [11], [12], but these approaches are very conservative in order to be reliable. The rapid change in RSS with WiFi diminishes the value in modeling an antenna's directionality which is why communications maintenance literature often assumes a disk model for communication between agents [4], [13], [14].

By decreasing the carrier frequency to the 30-60 MHz range, a communication signal can propagate farther and has reduced multipath levels [15] in physically complex environments between ground agents. Miniaturized antennas for lower VHF also have been developed and demonstrated for low power, moderate rate communications [16]. Recently, we demonstrated the feasibility of creating a robotic Yagi-Uda antenna array, a type of parasitic array, to increase signal gain at this frequency [1]. To form an array, antennas are spaced closely so that they mutually couple; passive antennas (i.e., unpowered), absorb or "parasitize" the energy of the active antenna and re-radiate this energy creating areas of constructive and destructive interference (i.e., gain). The arrangement of these antennas is shown in Fig. 2.

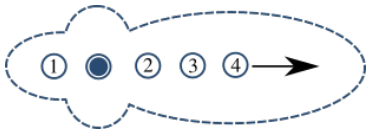

Fig. 2: Our robotic Yagi-Uda arrays are composed of an active antenna agent (solid circle) and passive antenna agents (numbered in the order in which they are added to increase gain). The arrow points in the direction of maximum gain of the array pattern (dashed line). An array with more passive antenna agents has higher gain when these antennas are optimally spaced.

In these low-VHF robotic arrays the robots are spaced 2-3 m; creating an array with one passive antenna increases range by 50 m in free-space [2]. The simple task of linearly aligning agents to create an array with significant directional gain is the motivation for the study of their application in robotic networks.

One could consider either sector visibility [17], [18] or range as an initial sensing model for communication between robotic arrays. While a sector is directional, it does not capture the continuous spatial variation in signal strength that occurs with changing orientation of an antenna array. In addition, in a graph of agents, a link formed by an agent in a sector visibility model is directed, where as links between parasitic arrays are undirected. Range based models (e.g., the disk model) on the other hand, are not directional but are often used for modeling radio propagation between robots. Researchers have used this model to develop formation stabilization, and consensus in groups of mobile autonomous agents [19], [20]. Multi-robot systems can also optimize their connectivity with respect to graph-theoretic metrics using a mix of graph-theoretic constraints and objectives [14], [21]. Variations allow the network to be more distributed [13], and more robust [4]. In this paper, we consider utilizing the multi-agent parasitic arrays as a means of enhancing directional gain to provide desired overall network properties.

III. Approach

We assume we have $n \in \mathbb{Z}$ computationally powerful UGVs which act as active antenna agents. In the sequel, we refer to the state of the robotic parasitic arrays and the state of the active antenna agents interchangeably. The states of these robotic agents are described in Table I. If these robotic parasitic arrays can communicate we assume they can jointly estimate each other's states in the same coordinate system using distributed SLAM [22] or another approach and model their radio propagation. The level of position uncertainty due to noise and gradual variation in signal strength due to large, signal-attenuating objects and buildings implies that some level of control is required to maintain communication.

Agents can create and control a directional signal if they form a parasitic antenna array. The range and directionality created by forming the array is gain with respect to a single omni-directional antenna on an active antenna agent. For simplicity, we assume each $i \in [0, n]$ agent has states $x_i, y_i \in \mathbb{R}^n$ defining agents' locations. Additionally, $\theta_i \in \mathbb{R}^n$ defines the direction of maximum array gain for each active antenna array. There is no assumption that the front of the agent or some set of sensors is aligned with the antenna array direction. This assumption partially decouples other tasks the active antenna agent may be engaged with from the connectivity maintenance task. As the positioning of the passive antenna agents controls the array orientation, the gain is controlled by these agents.

A. System Model and Problem Formulation

Passive antenna agents do not require a radio to alter the properties of the array so these robots can be flyers or some other agile, high-speed robot that has the appropriate electrical properties for forming a parasitic array. In an experiment the passive antenna agents would use WiFi radios

TABLE I: System States and Variables

n	number of active antenna robots (agents) which form robotic parasitic arrays (indexed by i,j)
θ_i	orientation of the array of active antenna robot i
ρ_i	parasitic effect of the array of active antenna robot i
q_i	$[x_i, y_i, \theta_i, \rho_i]$, the state of active antenna robot i
u_i	control for active antenna robot i
$P(q_i, q_j)$	Power received at active antenna robot i after transmission from active antenna robot j
$\phi(q_i, q_j)$	Bearing angle of active antenna robot j from active antenna robot i
G_i	Gain of the array of active antenna robot i which is receiving a signal, later defined as $G(\phi(q_i, q_j), q_{i,4})$
G_j	Gain of the array of active antenna robot j which is transmitting a signal, later defined as $G(\phi(q_j, q_i), q_{j,4})$

to communicate with the active antenna agents to coordinate array formation. The control and allocation of these passive antenna agents, as well as their ability to rendezvous to form arrays, is outside of the scope of this paper. We assume that the passive antenna robots will move and position as necessary, and describe their motion as a state of the robotic parasitic array. We call this state *parasitic effect* which is characterized by ρ_i, such that $\rho_i \in \mathbb{R}$ is related to the number of passive antenna agents in the array. To be clear, we are abstracting away the dynamics of the passive antenna agents by saying that the orientation and parasitic effect are states of the robotic array. The array state $q = [x, y, \theta, \rho]$ rows are indexed by i and the columns are indexed by $k \in \{1, 2, 3, 4\}$ so that $q \in \mathbb{R}^{n\times 4}$. The degrees of freedom, (x,y,θ,ρ), are independently actuated, and we assume a single-integrator dynamics model for the agents given by

$$\dot{q} = u. \tag{1}$$

In this equation, the control is $u \in \mathbb{R}^{n\times 4}$. This simple model is sufficient for solving the overall system control and passive antenna robot grouping with active antenna robots.

The Friis Transmission Equation (Eqn. 2) describes received power at active antenna agent i, $P(q_i, q_j)$, from another j active antenna agent where

$$P(q_i, q_j) = \frac{P_j G_j G_i c^2}{(4\pi R(q_i, q_j) f)^2}. \tag{2}$$

We assume that the transmit power P_j of agent j, speed of light c, and the antennas' center frequency f are constant. In our simulations we choose $P_j = 0.025$ W, $c =$ 3e8 m/s, and $f =$ 40e6 Hz for all agents. The distance between the two active antenna agents is $R(q_i, q_j) = \sqrt{((q_{i,1} - q_{j,1})^2 + (q_{i,2} - q_{j,2})^2)}$. Gains G_j and G_i are unitless multipliers of the transmitting antenna and the receiving antenna respectively.

The gain for robotic parasitic arrays is a function of q_i and q_j, thus G_i and G_j are not constant. Gain at agent i is a function of angle $\phi(q_i, q_j)$ from the direction of maximum gain of active antenna agent i ($\theta_i \equiv q_{i,3}$) to the relative bearing of agent j ($\tan^{-1}(\frac{q_{j,2}-q_{i,2}}{q_{j,1}-q_{i,1}})$).

$$\phi(q_i, q_j) = \tan^{-1}\left(\frac{q_{j,2} - q_{i,2}}{q_{j,1} - q_{i,1}}\right) - q_{i,3} \tag{3}$$

Next, let us approximate the beam pattern of an antenna array for 2 dimensions. The variable $G_i = G(\phi(q_i, q_j), q_{i,4})$ in parasitic antenna arrays cannot be described by a simple analytical model. Experimental studies [23] show that as more passive antennas are added, the gain increases, and the beam-width decreases. These results are shown in Table II.

For the purposes of control, we want to approximate the gain G_i as a function of $\phi(q_i, q_j)$ and ρ_i which is continuously differentiable. Normal distributions have been used to approximate gain patterns [24], but a normal distribution model is not differentiable from π to $-\pi$. A Tikhonov distribution, also known as a Von-Misses distribution, or the circular normal distribution, is continuously differentiable so we adopt this as a beam pattern model.

Another simplifying assumption is that passive antenna agents can configure to form sub-optimal configurations to achieve intermediate gain values. This is how we justify our assumption that $\rho_i \in \mathbb{R}$. The first order dynamics of ρ_i also help capture the time that it takes for an array to configure and achieve maximum gain. This relation between ρ_i and number of passive antenna agents implies that a parasitic effect of ρ_i requires $\lceil \rho_i \rceil$ passive antenna agents to form the array. When $\rho_i = 0$, this is a vacuous state of the robotic array i where there are no passive antenna agents; the "array" is an active antenna agent i. In this situation, the orientation is meaningless as the array has no orientation without passive antenna agents; the array orientation is also irrelevant as the active antenna agent radiates omni-directionally. We choose 6 as the maximum number of passive antenna agents that can participate in an array since there is a point of diminishing returns from adding additional passive antennas to a Yagi-Uda array. Therefore, $\rho_i \in [0, 6]$. The gain of the receiving antenna array in terms of state q is

$$G_i = G(\phi(q_i, q_j), q_{i,4}) = \frac{\exp((q_{i,4}/\alpha)\cos(\phi(q_i, q_j)))}{I_0(q_{i,4}/\alpha)}. \tag{4}$$

In Eqn 4 we have already multiplied the Tikhonov distribution by 2π, which cancels out 2π in the denominator. Here, I_0 is a Modified Bessel function of order zero. We find an appropriate value for α to roughly match Table II is $\alpha = 2.3$. When the parasitic effect is 0, the gain is 1 for all values of ϕ; this is the normalized radiation pattern for an omni-directional antenna. Note that other connectivity maintenance approaches using Fiedler value implement a communications model similar to Friis Transmission (Eqn. 2) with gain values in reception and transmission equal to 1.

The model in Eqn. 4 captures main lobe behavior, but does not capture the beam pattern's nulls or sidelobes. We did not add the additional complexity required to model side-lobes because they create areas of local maxima. Incorporating a multi-lobe beam pattern model is an interesting open problem.

Gain for a parasitic array is symmetric in reception and transmission. Denoting transmission gain as G_j, this is

TABLE II: Gain of a Yagi-Uda Parasitic Antenna Array

Passive Antennas	Gain (dB)	Gain	Beam Width (°)
0	0	1	–
1	5	1.8	66
2	7.5	2.4	57
3	8.5	2.6	
4	9.5	3.0	48
5	10.5	3.3	40
6	11.5	3.8	

simply G_i with i and j reversed, so $G_j = G(\phi(q_j, q_i), q_{j,4})$. With gain as a function of active antenna agent states for transmission from node j to receive node i, we can update the Friis transmission equation to obtain

$$P(q_i, q_j) = \frac{P_j G(\phi(q_i, q_j), q_{i,4}) G(\phi(q_j, q_i), q_{j,4}) c^2}{(4\pi R(q_i, q_j) f)^2}. \quad (5)$$

This final version of Eqn. 2 is now in terms of our active antenna agent states q. Now that we can approximate the power of a communication connection, we can model the connection quality between agents.

B. Graph of Agent Connectivity

We relate the received power to communications between the agents and then observe the group connectivity within a graph structure. The values in the adjacency matrix $A(q) \in \mathbb{R}^{n \times n}$ are the weights of the edges of the graph corresponding to the agent i's ability to receive data from agent j. An agent's radio must be able to disambiguate the signal from the noise in the environment. This noise sets a threshold for power, P_{low}, below which there is no connection. There is also a power level, P_{high}, above which there is no increase in data received. These values are relative to the specific radio technology. From prior work we find $P_{high} = -45$ dB and $P_{low} = -70$ dB are reasonable values and we adopt these for our simulation [25]. In addition, the large variation in signal strength leads us to favor measuring signal strength in decibels instead of watts defined as $P_{dB}(q_i, q_j) = 10 \log_{10}(P(q_i, q_j))$. Using Eqn. 5 we can create a model of connectivity from agent i to agent j given by

$$A(q)_{i,j} = \begin{cases} 0 & i = j \\ 0 & \frac{P_{dB}(q_i,q_j) - P_{low}}{P_{high} - P_{low}} < 0, i \neq j \\ 1 & \frac{P_{dB}(q_i,q_j) - P_{low}}{P_{high} - P_{low}} \geq 1, i \neq j \\ \frac{P_{dB}(q_i,q_j)) - P_{low}}{P_{high} - P_{low}} & \text{o.w.} \end{cases} \quad (6)$$

If the power received at agent i is at or above P_{high}, the connectivity is 1. If the power received at agent i is less than P_{low} we say the connectivity along that edge is 0. An agent cannot form an edge with itself, therefore $A(q)_{i,j} = 0$ when $i = j$. As per this definition, $A(q)_{i,j}$, is piece-wise continuous.

In Fig. 3 we show how the connectivity varies as one agent moves around another fixed at $(0, 0)$ using this model. The agents maintain a fixed orientation of $\theta_i = 0$ and a constant parasitic effect. Agent j has $\rho_j = 0$ (i.e., an omni-directional antenna) and agent i has $\rho_i = 6$ (i.e., it is highly directional with 6 passive antenna agents forming an array). With these values, when the antenna array agents are spaced by 20 m with each other there is perfect communication. As the agents move farther apart the communication decreases until communication is lost.

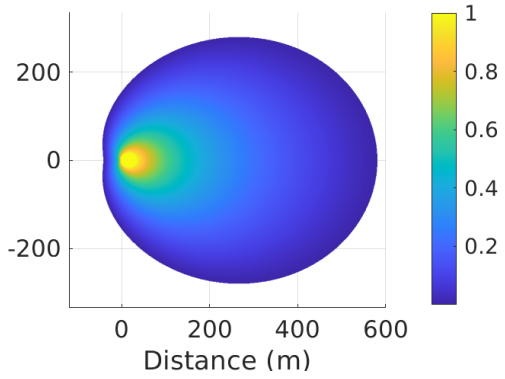

Fig. 3: Communication between agent i, located at (0,0), and agent j in different (x, y) positions, both with fixed values of θ and ρ.

C. Fiedler Optimization

The Fiedler value, a graph-theoretic metric of connectivity of a multi-agent system, is a function of the adjacency matrix $A(q)$. When the Fiedler value is greater than zero, there exists a path along edges of the graph connecting any pair of agents. The existence of a communication path means that there is connectivity between all agents in the group. The gain in reception is the same in transmission, so the adjacency matrix is symmetric. The values of $P_{dB}(q_i, q_j)$ are all positive, therefore $A(q)_{i,j} \geq 0$. The degree of each node as $D(q)_{ii} = \sum_{j=1}^{n} A(q)_{i,j}$ where $D(q) \in \mathbb{R}^{n \times n}$. The Laplacian $L(q) \in \mathbb{R}^{n \times n}$ is defined as $L(q) = A(q) - D(q)$. It is positive semidefinite as it is symmetric and all of its eigenvalues are non-negative. The Fiedler value λ_2 is the second smallest eigenvalue of the Laplacian; the smallest eigenvalue is always zero.

The overall control objective is to configure the agents and parasitic elements to maximize the connectivity of the network. This goal, when expressed through the Fiedler value, is given as

$$\max_{q} \quad \lambda_2(L(q)) \quad (7)$$

Note that given the 4 degrees of freedom for each robotic array, we have created a non-convex optimization problem. There are multiple maxima when optimizing connectivity between active antenna agents. Agents can maneuver to decrease their relative distance or increase their gain. This creates an interesting set of trade-offs based on the speed of active antenna agents, the availability of passive antenna agents, and the time required to form and optimize an antenna array.

In [13], [21], [14] the authors formulate a subgradient method for increasing Fiedler value. We follow the definition of Fiedler value as described in [13] as

$$\begin{aligned}\lambda_2(L(q)) &= \inf_{p\perp\mathbf{1},p\neq 0} \frac{p^T L(q) p}{p^T p} \\ &= \inf_{p\perp\mathbf{1},p\neq 0} \frac{\sum_i^n \sum_j^n A(q)_{i,j}||p_i - p_j||_2^2}{p^T p},\end{aligned} \tag{8}$$

where $\mathbf{1} \in 1^n$ is a vector of size n and p is any unit vector. In this equation we replace p with v_2, the normalized ($||v_2|| = 1$) left eigenvector corresponding to the Fiedler value.

The differential of λ_2, is

$$\begin{aligned}\frac{\partial \lambda_2(L(q))}{\partial q_{i,k}} &= \frac{\partial v_2^T L(q) v_2}{\partial q_{i,k}} \\ &= \frac{\partial v_2^T}{\partial q_{i,k}} L(q) v_2 + v_2^T \frac{\partial L(q)}{\partial q_{i,k}} v_2 + v_2^T L(q) \frac{\partial v_2}{\partial q_{i,k}}.\end{aligned} \tag{9}$$

Since $L(q)^T = L(q)$, it follows that

$$\begin{aligned}v_2^T L(q) \frac{\partial v_2}{\partial q_{i,k}} &= \frac{\partial v_2^T}{\partial q_{i,k}} L(q) v_2 = \lambda_2 \frac{\partial v_2^T}{\partial q_{i,k}} v_2 \\ &= \frac{1}{2}\frac{\partial v_2^T v_2}{\partial q_{i,k}} = \frac{1}{2}\frac{\partial ||v_2||^2}{\partial q_{i,k}} = 0.\end{aligned} \tag{10}$$

Following Eqn.10 certain terms in Eqn. 9 are zero; we can determine a simpler relationship [13].

$$u_{i,k} = \dot{q}_{i,k} = \frac{\partial \lambda_2}{\partial q_{i,k}} = v_2^T \frac{\partial L(q)}{\partial q_{i,k}} v_2 \tag{11}$$

From Eqn 11 it follows that the control for each agent is

$$u_{i,k} = v_2^T \frac{\partial L(q)}{\partial q_{i,k}} v_2 = \left(\sum_j^n \frac{\partial A(q)_{i,j}}{\partial q_{i,k}} (v_{2,i} - v_{2,j})^2 \right). \tag{12}$$

Here, i and j are indexing the eigenvector v_2. Using this controller, agents are able to improve communication of the system. As in, [13], [14] we are implementing a subgradient approach to control agents to maximize the Fiedler value. Agents implementing this controller will always improve global communication capability of the group; however, since this is a subgradient approach the controller does not guide the robots on the most efficient trajectory towards better communication.

The partial derivative of the adjacency matrix is

$$\frac{\partial A(q)_{i,j}}{\partial q_{i,k}} = \frac{10}{\ln(10) P(q_i, q_j)(P_{high} - P_{low})} \times \frac{\partial P(q_i, q_j)}{\partial q_{i,k}} \tag{13}$$

where $\ln$ is the natural logarithm. The derivative $\frac{\partial A(q)_{i,j}}{\partial q_{i,k}}$ exists everywhere that a link is sub-optimal. It follows that $\frac{\partial A(q)_{i,j}}{\partial q_{i,k}} = 0$ when $A(q)_{i,j} = 1$ as the link between i and j cannot be improved. The derivation of $\frac{\partial P(q_i,q_j)}{\partial q_{i,k}}$ is given in the Appendix.

D. Maintaining Connectivity While Pursuing Other Objectives

We make a small change to our system model to incorporate other control inputs. These inputs may be used to guide the translational control of active antenna agents to other control objectives. Thus we update the system model to include this additional controller given by

$$\dot{q} = u + \hat{u} \tag{14}$$

where $\hat{u} \in \mathbb{R}^{n\times 4}$. The control $\hat{u}$ must have additional constraints so that our control formulation can maintain communication. First, $\hat{u}_{i,3} = \hat{u}_{i,4} = 0$ for all i. We must also maintain that the translational control component of $\hat{u}$ (i.e., $\hat{u}_{i,1}$ and $\hat{u}_{i,2}$) must be bounded as described in [4]. As in [4], we modify our controller defined in Eqn. 12 with the addition of $\mathrm{csch}^2(\lambda_2 - \epsilon)$, where

$$\begin{aligned}u_{i,k} &= \mathrm{csch}^2(\lambda_2 - \epsilon) v_2^T \frac{\partial L}{\partial q_{i,k}} v_2 \\ &= \mathrm{csch}^2(\lambda_2 - \epsilon) \left(\sum_j^n -\frac{\partial A(q)_{i,j}}{\partial q_{i,k}} (v_{2,i} - v_{2,j})^2 \right).\end{aligned} \tag{15}$$

In this equation, $\epsilon \in \mathbb{R}$ is a lower bound for the Fiedler value. Since $\mathrm{csch}^2(\lambda_2 - \epsilon)$ approaches infinity as λ_2 approaches ϵ, the magnitude of control for communication becomes large when $\lambda_2 - \epsilon \to 0$, guaranteeing that the system maintains at least this value of global connectivity. Note, $\epsilon < \lambda_2$ at the beginning of every trial. Since the control for other objectives ($\hat{u}$) is bounded, the control for maintaining communication u will always be larger than $\hat{u}$ as the Fiedler value approaches ϵ.

IV. SIMULATIONS

We compare our controller from Eqn. 15 with the standard approach of moving to increase Fiedler value in the absence of other controllers. Then, we show the capability to form parasitic arrays to enable operation at extended range when $\hat{u}_i$ is pulling two arrays apart. For our simulations to execute we must make some additional considerations. First we alter Eqn. 14 to be $\dot{q} = u\mathrm{diag(h)} + \hat{u}$. This scaling factor $h \in \mathbb{R}^4$, $h_k > 0$, does not affect our previous discussions about how the controller maximizes the Fiedler value or the ability of the controller to overcome the bounded control input $\hat{u}$. It compensates for the discrepancy in magnitude between the state positions x and y, the orientation θ, and parasitic effect ρ. Another way to view h is as a parameter capturing the an arrays' ability to move, re-orient, or form an array. We set the parameter $h = [200, 200, 1, 1]$ for a scenario where active ground antenna robots move slowly relative to flying passive antenna robots.

Another practical question is how to overcome saddle points in our optimization. When $\rho_i \equiv q_{i,4} = 0$, saddle points exist for our sub-gradient method controlling orientation. From Eqn. 21 we can see that $\rho_i = 0$ results in $\frac{\partial A(q)_{i,j}}{\partial \theta_i} = 0$. This is a problem when the array is facing away from the

optimal direction where $\frac{\partial A(q)_{i,j}}{\partial q_{i,4}} < 0$. We assume the passive antenna robot UAVs can fly directly over the active ground antenna robot in response to this negative value to change orientation by π radians when $\frac{\partial A(q)_{i,j}}{\partial q_{i,4}} < 0$ and $\rho_i = 0$. As a result, there are discontinuities in orientation but these discontinuities occur only when $\rho_i = 0$ for a given i. Other saddle points may be present, however in simulation, the controller escaped them.

A. *Verifying Communications Maintenance*

We compare active antenna agents which can acquire up to 6 passive antenna agents with the case when active antenna agents do not have passive antenna agents. In the single active antenna agent case, the beam pattern is uniform omni-directional; therefore it is implementing a disk connectivity model approach. In both cases, we initialize the simulation with $n = 4$ active agents, $q_1 = [-100, 0, 0, 0]$, $q_2 = [100, 0, 0, 0]$, $q_3 = [-50, 25, 0, 0]$, $q_4 = [50, -25, 0, 0]$. We set $\hat{u}_i = [0, 0, 0, 0]$ to test Fiedler maximization without other controllers present. Initially, all of the agents share an edge (i.e., $A(q)_{i,j} > 0, i \neq j$). We set time step $d_t = 0.4$ s and $\epsilon = 0$. For active antenna agents which cannot form parasitic antenna arrays, we set $\rho_i = 0$ regardless of the control input; mathematically, this is the same as the disk model approach described in [4]. The parasitic effect of all agents in both cases is initially zero. In Fig. 4 we show the trajectories of both approaches (with and without array forming). Interestingly, in both cases the agents follow the same paths to maximize Fiedler value but the agents which cannot form arrays are controlled to move closer together than the agents which can form arrays. Similarly, in Fig. 5 our approach achieves a higher Fiedler value in the same amount of time than the agents which cannot form arrays.

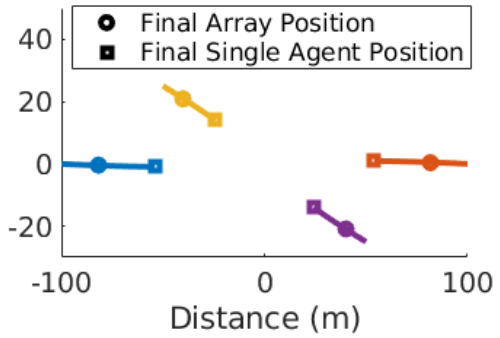

Fig. 4: Trajectories of active antenna agents. Square markers denote the final positions of the single, non-array-forming agents which employ a disk model. Circle markers denote the final positions of the array forming active antenna agents.

This difference in final position and Fiedler value demonstrates that if the agents can form arrays, they will always outperform existing Fiedler maximization approaches which assume a disk model. The array forming capability allows these array forming agents to have a higher Fiedler value than the more closely spaced agents which cannot form arrays. If an active antenna agent can easily form an antenna array, communications links between two active antenna agents can be improved far more quickly than if the agents were to drive towards each other.

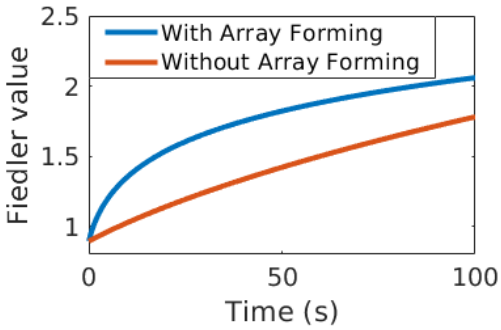

Fig. 5: Fiedler value over time for both trials of agents shown in Fig. 4.

Another interesting feature of our array forming approach is where active antenna agents form arrays of different sizes. In Fig. 6 we plot the parasitic effect of the agents which are able to form antenna arrays from the comparison trial shown in Fig 4. Agents 1 (blue) and 2 (red) form larger arrays than agents 3 (yellow) and 4 (purple). As the parasitic effect increases, the beam pattern is more directional. When arrays become more directional, overall connectivity might be reduced by weakening links which are not in the direction of maximum gain. Our subgradient approach is sensitive to this through the summation of link gradients in Eqn. 15. As a result, active agents stabilize their arrays at a certain size. Similarly, antenna arrays should have more directional beam patterns when the agents it has links to are confined to a smaller angular range. This angular distribution is more confined when agents are farther from the centroid of the array forming agents. Consequently, the active antenna agents form larger arrays at larger distances and, hence agents 1 and 2 form larger arrays than agents 3 and 4.

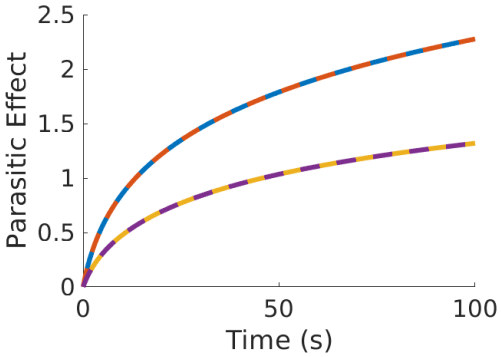

Fig. 6: Parasitic effect (ρ) of the 4 arrays over time. The plot colors match the agents' colors from trajectories in Fig.4 ending with the circle marker.

B. *Effects of Array Forming on Operational Range*

We constructed a simple scenario where there are two active antenna agents with $\hat{u_1} = [-5, 0, 0, 0]$ and $\hat{u_2} =$

$[5,0,0,0]$ in order to determine the effects of array forming on operational range. This controller $\hat{u}$ causes the active antenna agents to drive away from each other but our communication maintenance controller u maintains communication between the active antenna agents. These agents begin on the x-axis ($q_1 = [-50,0,0,0], q_2 = [50,0,0,0]$). From this initial configuration we run 13 tests. We consider up to 12 agents divided between 2 active antenna agents for forming parasitic arrays. If there is an even number of passive antenna agents in the trial, the passive antenna agents are divided equally between active antenna agents 1 and 2. If there is an odd number of passive antenna agents, agent 1 is allowed 1 more than agent 2. All parameters are the same as in earlier simulations. The results of this set of tests can be seen in Fig. 7.

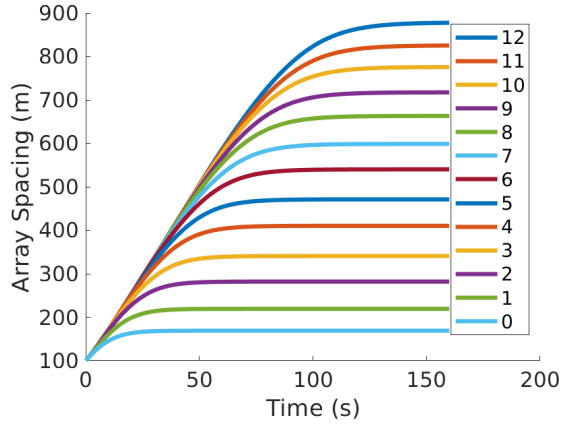

Fig. 7: Maximum distance between 2 active antenna agents which form parasitic arrays. Each plot corresponds the number of passive agents available to form arrays.

These results demonstrate that there is a range benefit with the addition of each successive passive antenna agent in this simple scenario with only 2 active antenna agents. At the end of the test, all of the arrays have reached an equilibrium between u and $\hat{u}$ controllers. This equilibrium is between u pushing the active antenna agents closer together to maintain good communication and $\hat{u}$ pulling the active antenna agents apart.

V. CONCLUSION AND FUTURE WORK

We described a new model for extending the range of reliable, long-range, low-VHF communication signals. This was accomplished by developing a controller for a robotic array which optimized and appropriately defined a graph-theoretic metric. Our simulations demonstrated that array forming is more useful for improving communication when passive agent motion is less costly than active agent motion, and when traversing the environment is difficult. As a result, this capability should be especially useful in indoor and urban environments where walls induce movement constraints. An additional advantage of using this approach in these complex environments is that the low-VHF signal created by forming the array is more reliable at longer range than when compared with microwave radio frequency operation such as WiFi. Parasitic array formation also becomes more valuable as the cost of radios powering the active antennas become more expensive.

There are a number of things we could explore further. First, we could make parasitic array formation more realistic by accounting for the motion constraints imposed by indoor and urban environments. This would mean passive antenna agents take time to transfer into and out of parasitic arrays, and constrain robotic array orientation. Adding these complexities would allow us to investigate trade-offs in mission time and motion capabilities. Adding constraints based on the availability of passive antenna agents is another consideration. The ability of passive antenna agents to become active and therefore nodes in the graph is another interesting research avenue.

VI. APPENDIX

Here, we find the partial derivative of the power with respect to the each of the 4 state variables for agent i as required by Eqn 13. The gain functions are written as $G_i = G(\phi(q_i,q_j),q_{i,4})$ and $G_j = G(\phi(q_j,q_i),q_{j,4})$ to make the following equations easy to read.

$$\frac{\partial P(q_i,q_j)}{\partial q_{i,k}} = \frac{P_j c^2}{(4\pi f)^2}\left(\frac{R(q_i,q_j)^2 \times \frac{\partial}{\partial q_{i,k}}(G_i G_j))}{(R(q_i,q_j)^2)^2} - \frac{(G_i G_j) \times \frac{\partial R(q_i,q_j)^2}{\partial q_{i,k}}}{(R(q_i,q_j)^2)^2}\right), k = \{1,2,3,4\} \tag{16}$$

This function is defined for all 4 state variables of active antenna agent i (i.e., $k = \{1,2,3,4\}$).

Let us focus on the x and y states where $k = 1$ is the x component and $k = 2$ is the y component. Here, $R(q_i,q_j)$ is a function of states x_i and y_i.

$$\frac{\partial (R(q_i,q_j)^2)}{\partial q_{i,k}} = 2(q_{i,k} - q_{j,k}), k = \{1,2\} \tag{17}$$

Eqn. 16 for $k = 1,2$ is simplified in Eqn. 18

$$\frac{\partial P(q_i,q_j)}{\partial q_{i,k}} = \frac{P_j c^2}{(4\pi R(q_i,q_j) f)^2} \times \left(\frac{\partial}{\partial q_{i,k}}(G_i G_j) - \frac{2(q_{i,k} - q_{j,k})(G_i G_j)}{R(q_i,q_j)^2}\right), k = \{1,2\} \tag{18}$$

As G_i and G_j are functions of all the state variables we must take the partial derivative of the product of these functions.

$$\frac{\partial}{\partial q_{i,k}}(G_i G_j) = \frac{\partial G_i}{\partial q_{i,k}} G_j + G_i \frac{\partial G_j}{\partial q_{i,k}}, k = \{1,2,3,4\} \tag{19}$$

$$\frac{\partial G_i}{\partial q_{i,k}} = \frac{\partial G(\phi(q_i,q_j),q_{i,4})}{\partial \phi(q_i,q_j)} \frac{\partial \phi(q_i,q_j)}{\partial q_{i,k}}, k = \{1,2,3,4\} \tag{20}$$

Where, $\phi(q_i,q_j)$ is a function of the positions of agents i and j and the orientation of agent j. When the variable $k = 3$,

this corresponds the orientation and $k = 4$ corresponds to the parasitic effect. The parasitic effect of either array has no affect on $\phi(q_i, q_j)$, so it follows that

$$\frac{\partial G(q_i,q_j)}{\partial \phi(q_i,q_j)} = -(q_{i,4}/\alpha)\sin(\phi(q_i,q_j)) \times \frac{\exp((q_{i,4}/\alpha)\cos(\phi(q_i,q_j))}{I_0(q_{i,4}/\alpha)}, k = \{1,2,3\} \tag{21}$$

and

$$\frac{\partial \phi(q_i,q_j)}{\partial q_{i,k}} = \frac{q_{j,k} - q_{i,k}}{R(q_i,q_j)^2}, k = \{1,2\}. \tag{22}$$

After substituting Eqn. 21 and Eqn. 22 into Eqn. 20 we have the partial derivative of G_i. Note that these equations can be used to find G_j by transposing i and j as shown in Eqn. 23.

$$\frac{\partial G_j}{\partial q_{i,k}} = \frac{\partial G(\phi(q_j,q_i),q_{j,4})}{\partial \phi(q_j,q_i)} \frac{\partial \phi(q_j,q_i)}{\partial q_{i,k}} \tag{23}$$

We now have all of the necessary components to determine the values of Eqn. 18 for $k = 1, 2$. Now, let us look at the partial derivatives with respect to orientation and parasitic affect. In Eqn 18, only $G_i = G(\phi(q_i, q_j), q_{i,4})$ is a function of $q_{i,3}$ or $q_{i,4}$. As a result, several terms drop out as the partial derivatives of $R(q_i, q_j)$ and G_j with respect to $q_{i,3}$ and $q_{i,4}$ are both zero.

$$\frac{\partial P(q_i,q_j)}{\partial q_{i,k}} = \frac{P_j c^2}{(4\pi R(q_i,q_j) f)^2} \frac{\partial G_i}{\partial q_{i,k}} G_j, k = \{3,4\} \tag{24}$$

Eqn. 21 and 22 can be substituted into this equation. Knowing that $\partial\phi(q_i, q_j)/\partial q_{i,3} = -1$, we can solve Eqn. 24 for $k = 3$. Finally, we need the partial derivative of G_i with respect to the parasitic effect $q_{i,4}$ to solve solve Eqn. 24 for $k = 4$.

$$\frac{\partial G_i}{\partial q_{i,4}} = \frac{1}{\alpha}\exp(q_{i,4}/(\alpha\cos(\phi(q_i,q_j)) \times \left(\frac{I_0(q_{i,4}/\alpha)\cos(\phi(q_i,q_j)) - I_1(q_{i,4}/\alpha)}{I_0(q_{i,4}/\alpha)^2}\right) \tag{25}$$

This completes the derivation of values in Eqn. 13.

VII. ACKNOWLEDGMENT

Thanks to Andoni Aguirrezabal and Yoichiro Endo of Intelligent Automation Inc. for their visualization software support.

REFERENCES

[1] F. T. Dagefu, J. N. Twigg, C. R. Rao, and B. M. Sadler, "Directional communication enabled by mobile parasitic elements," in *2019 International Conference on Military Communications and Information Systems (ICMCIS)*. IEEE, 2019, pp. 1–7.

[2] J. Twigg, F. Dagefu, N. Chopra, and B. M. Sadler, "Robotic parasitic array optimization in outdoor environments," in *2019 IEEE International Symposium on Safety, Security, and Rescue Robotics (SSRR)*. IEEE, 2019, pp. 1–8.

[3] J. Fink, A. Ribeiro, and V. Kumar, "Motion planning for robust wireless networking," in *Robotics and Automation (ICRA), 2012 IEEE International Conference on*. IEEE, 2012, pp. 2419–2426.

[4] L. Sabattini, C. Secchi, N. Chopra, and A. Gasparri, "Distributed control of multirobot systems with global connectivity maintenance," *IEEE Transactions on Robotics*, vol. 29, no. 5, pp. 1326–1332, 2013.

[5] G. Hollinger and S. Singh, "Multi-robot coordination with periodic connectivity," in *2010 IEEE International Conference on Robotics and Automation*. IEEE, 2010, pp. 4457–4462.

[6] N. Tantubay, D. R. Gautam, and M. K. Dhariwal, "A review of power conservation in wireless mobile adhoc network (manet)," *International Journal of Computer Science Issues (IJCSI)*, vol. 8, no. 4, p. 378, 2011.

[7] R. J. Marcotte and E. Olson, "Adaptive forward error correction with adjustable-latency qos for robotic networks," in *Robotics and Automation (ICRA), 2016 IEEE International Conference on*. IEEE, 2016, pp. 5283–5288.

[8] N. Kumari, R. Kumar, and R. Bajaj, "Energy efficient communication using reconfigurable directional antenna in manet," *Procedia Computer Science*, vol. 125, pp. 194–200, 2018.

[9] G. Astudillo and M. Kadoch, "Neighbor discovery and routing schemes for mobile ad-hoc networks with beamwidth adaptive smart antennas," *Telecommunication Systems*, vol. 66, no. 1, pp. 17–27, 2017.

[10] B. Kusy, D. Abbott, C. Richter, C. Huynh, M. Afanasyev, W. Hu, M. Brünig, D. Ostry, and R. Jurdak, "Radio diversity for reliable communication in sensor networks," *ACM Transactions on Sensor Networks (TOSN)*, vol. 10, no. 2, p. 32, 2014.

[11] E. Stump, N. Michael, V. Kumar, and V. Isler, "Visibility-based deployment of robot formations for communication maintenance," in *2011 IEEE international conference on robotics and automation*. IEEE, 2011, pp. 4498–4505.

[12] Y. Kantaros, M. Thanou, and A. Tzes, "Distributed coverage control for concave areas by a heterogeneous robot–swarm with visibility sensing constraints," *Automatica*, vol. 53, pp. 195–207, 2015.

[13] P. Yang, R. A. Freeman, G. J. Gordon, K. M. Lynch, S. S. Srinivasa, and R. Sukthankar, "Decentralized estimation and control of graph connectivity for mobile sensor networks," *Automatica*, vol. 46, no. 2, pp. 390–396, 2010.

[14] E. Stump, A. Jadbabaie, and V. Kumar, "Connectivity management in mobile robot teams," in *2008 IEEE international conference on robotics and automation*. IEEE, 2008, pp. 1525–1530.

[15] F. T. Dagefu, J. Choi, M. Sheikhsofla, B. M. Sadler, and K. Sarabandi, "Performance assessment of lower vhf band for short range communication and geolocation applications," *Radio Science*, vol. 50, no. 5, May 2015.

[16] J. Choi, F. T. Dagefu, B. M. Sadler, and K. Sarabandi, "Electrically small folded dipole antenna for hf and low-vhf bands," *IEEE Antennas and Wireless Propagation Letters*, vol. 15, pp. 718–721, 2016.

[17] J. Yu, S. M. LaValle, and D. Liberzon, "Rendezvous without coordinates," *IEEE Transactions on Automatic Control*, vol. 57, no. 2, pp. 421–434, 2011.

[18] H. A. Poonawala and M. W. Spong, "On maintaining visibility in multi-robot-networks with limited field-of-view sensors," in *2017 American Control Conference (ACC)*. IEEE, 2017, pp. 4983–4988.

[19] M. M. Zavlanos and G. J. Pappas, "Controlling connectivity of dynamic graphs," in *Proceedings of the 44th IEEE Conference on Decision and Control*. IEEE, 2005, pp. 6388–6393.

[20] M. C. De Gennaro and A. Jadbabaie, "Decentralized control of connectivity for multi-agent systems," in *Proceedings of the 45th IEEE Conference on Decision and Control*. IEEE, 2006, pp. 3628–3633.

[21] M. M. Zavlanos, M. B. Egerstedt, and G. J. Pappas, "Graph-theoretic connectivity control of mobile robot networks," *Proceedings of the IEEE*, vol. 99, no. 9, pp. 1525–1540, 2011.

[22] S. Choudhary, L. Carlone, C. Nieto, J. Rogers, Z. Liu, H. I. Christensen, and F. Dellaert, "Multi robot object-based slam," in *International Symposium on Experimental Robotics*. Springer, 2016, pp. 729–741.

[23] P. Viezbicke and Y. A. Design, "Nbs technical note 688," *US Government Printing Office, Washington, DC*, 1976.

[24] A. Haydar Lazem Al-Saadi, "Approximation of antenna patterns by means of a combination of gaussian beams," 2012.

[25] J. N. Twigg, J. R. Fink, P. L. Yu, and B. M. Sadler, "Efficient base station connectivity area discovery," *The International Journal of Robotics Research*, vol. 32, no. 12, pp. 1398–1410, 2013.